

Dark Matter Constraints from a Cosmic Index of Refraction

Susan Gardner^{1,2*} and David C. Latimer²

¹*Center for Particle Astrophysics and Theoretical Physics Department,
Fermi National Accelerator Laboratory, Batavia, IL 60510 and*

²*Department of Physics and Astronomy,
University of Kentucky, Lexington, KY 40506-0055*

Abstract

The dark-matter candidates of particle physics invariably possess electromagnetic interactions, if only via quantum fluctuations. Taken en masse, dark matter can thus engender an index of refraction which deviates from its vacuum value. Its presence is signaled through frequency-dependent effects in the propagation and attenuation of light. We discuss theoretical constraints on the expansion of the index of refraction with frequency, the physical interpretation of the terms, and the particular observations needed to isolate its coefficients. This, with the advent of new opportunities to view gamma-ray bursts at cosmological distance scales, gives us a new probe of dark matter and a new possibility for its direct detection. As a first application we use the time delay determined from radio afterglow observations of distant gamma-ray bursts to realize a direct limit on the electric-charge-to-mass ratio of dark matter of $|\varepsilon|/M < 1 \times 10^{-5} \text{ eV}^{-1}$ at 95% CL.

arXiv:0904.1612v4 [hep-ph] 8 Jun 2010

* Permanent Address

Some twenty-three percent of the Universe’s energy budget is in dark matter [1–3], yet, despite its abundance, little is known of its properties. A number of methods have been proposed for the detection of dark matter. Such studies typically rely, for direct searches, on dark-matter–nucleus scattering, and, for indirect searches, on two-body annihilation of dark-matter to Standard Model (SM) particles; constraints follow from the nonobservation of the aftermath of particular two-body interactions. In contrast, we probe dark matter in bulk to infer constraints on its particulate nature.

We search for dark matter by studying the modification of the properties of light upon passage through it. One can study either polarization [4] or propagation effects; we focus here on the latter. The resulting constraints are most stringent if dark matter consists of sufficiently low mass particles, be they, e.g., warm thermal relics or axion-like particles, that its number density greatly exceeds that of ordinary matter. We thus consider dark *matter*. Matter effects are signaled by dispersive effects in the speed or attenuation of light. We study this by introducing an index of refraction $n(\omega, z)$, whose deviation from unity is controlled by the light–dark-matter scattering amplitude in the forward direction, i.e., the forward Compton amplitude, as well as by the angular frequency ω of the light and the redshift z at which the matter is located. A dark-matter particle need not have an electric charge to scatter a photon; it need only couple to virtual electromagnetically charged particles to which the photons can couple. The scattering amplitude is related by crossing symmetry to the amplitude for dark-matter annihilation into two photons, so that any dark-matter model which gives rise to an indirect detection signal in the two-photon final-state [5] can also drive the index of refraction of light from unity. Its real part is associated with the speed of propagation, and we search for its deviation from unity by searching for frequency-dependent time lags in the arrival of pulses from distant gamma-ray bursts (GRBs).

The limits on the non-observation of frequency-dependent effects in the speed of light are severe. The best limits from terrestrial experiments control the variation in the speed of light c with frequency to $|\delta c|/c \lesssim 1 \times 10^{-8}$ [6], but the astrophysical limits are much stronger. The arrival time difference of pulses from the Crab nebula bound $|\delta c|/c \lesssim 5 \times 10^{-17}$ [7, 8], and still better limits come from the study of GRBs [8, 9]. GRBs are bright, violent bursts of high-energy photons lasting on the order of thousandths to hundreds of seconds, and their brightness makes them visible at cosmological distances. Time delays which are linear in the photon energy can occur *in vacuo* in theories of quantum gravity; the special features of GRBs make them particularly well-suited to searches for such signatures of Lorentz violation [9]. The detection of photons of up to ~ 31 GeV in energy from GRB 090510 severely constrains this scenario, placing a lower limit on the energy scale at which such linear energy dependence occurs to $1.2 E_{\text{Planck}} \approx 1.5 \times 10^{19}$ GeV [10]. Although vacuum Lorentz violation and light–dark-matter interactions can each induce dispersive effects, their differing red shift and frequency dependence render them distinct.

A model-independent analysis of the deviation of the refractive index from unity is possible if we assume that the photon energy is small compared to the energy threshold required to materialize the electromagnetically charged particles to which the dark matter can couple. In models of electroweak-symmetry breaking which address the hierarchy problem, a dark-matter candidate can emerge as a by-product. In such models the inelastic threshold ω_{th} is commensurate with the weak scale, or crudely with energies in excess of $\mathcal{O}(200 \text{ GeV})$, as the new particles are produced in pairs. If the photon energy ω satisfies the condition $\omega \ll \omega_{\text{th}}$, we can apply the techniques of low-energy physics to the analysis of the forward Compton amplitude. Under an assumption of Lorentz invariance and other symmetries, we

expand the forward Compton amplitude in powers of ω and give a physical interpretation to the coefficients of the first few terms as $\omega \rightarrow 0$ [11–13]. In particular, the term in $\mathcal{O}(\omega^0)$ is controlled by the dark matter particles’ charge and mass, weighted by preponderance, irrespective of all other considerations save our assumption of Lorentz invariance [14].

The relationship between the index of refraction $n(\omega)$ and the forward scattering amplitude $f_\omega(0)$ for light of angular frequency ω is well-known [15, 16], where we relate $f_\omega(0)$ to the matrix element \mathcal{M} of quantum field theory to connect to particle physics models of dark matter. Using standard conventions [17], we determine $n(\omega) = 1 + (\rho/4M^2\omega^2)\mathcal{M}_r(k, p \rightarrow k, p)$, in the matter rest frame [15], so that $p = (M, \mathbf{0})$ and $k = (\omega, \omega\hat{\mathbf{n}})$ with ρ the mass density of the scatterers and M the particle mass. In our analysis we assume $M \gg T(z)$, where $T(z)$ is the temperature of the dark matter at the red shift of the observed gamma-ray burst. Since $T(z)$ should be a factor of some $((1+z)/(1+z_{\text{prod}}))^{1-2}$ smaller than $T(z_{\text{prod}})$ at the moment of its production or decoupling, our limits are not restricted to cold dark matter exclusively. Moreover, even in the latter case, the candidate mass can be as light, e.g., as light as $M \sim 6 \times 10^{-6}$ eV in the axion model with Bose-Einstein condensation of Ref. [18]. Under the assumptions of causality or, more strictly, of Lorentz invariance, as well as of charge-conjugation, parity, and time-reversal symmetry in the photon–dark-matter interaction, we have [11, 13] $\mathcal{M}_r(k, p \rightarrow k, p) = f_1(\omega)\boldsymbol{\epsilon}'^* \cdot \boldsymbol{\epsilon} + if_2(\omega)\mathcal{S} \cdot \boldsymbol{\epsilon}'^* \times \boldsymbol{\epsilon}$, where \mathcal{S} is the spin operator associated with the dark-matter particle and $\boldsymbol{\epsilon}$ ($\boldsymbol{\epsilon}'$) is the polarization vector associated with the photon in its initial (final) state. The functions $f_1(\omega)$ and $f_2(\omega)$ are fixed in terms of the dark-matter electric charge and magnetic moment, respectively, as $\omega \rightarrow 0$ [14, 19, 20] without further assumption — it does not even matter if the dark-matter particle is composite. The amplitude $\mathcal{M}_r(k, p \rightarrow k, p)$ is implicitly a 2×2 matrix in the photon polarization, and its diagonal matrix elements describe dispersion in propagation and attenuation [16]. The $f_2(\omega)$ term describes changes in polarization with propagation, so that we need not consider it further. Under analyticity and unitarity, expanding $f_1(\omega)$ for $\omega \ll \omega_{\text{th}}$ yields a series in positive powers of ω^2 for which the coefficient of every term of $\mathcal{O}(\omega^2)$ and higher is positive definite [11, 12]. Thus a term in $n(\omega)$ which is linear in ω , discussed as a signature of Lorentz violation [9, 21], does not appear if $\omega < \omega_{\text{th}}$ and the medium is unpolarized. We parametrize the forward Compton amplitude as $\mathcal{M}_r = \sum_{j=0} A_{2j}\omega^{2j}$, where $A_0 = -2\varepsilon^2 e^2$ [14, 17] and the dark-matter millicharge is εe . The terms in $\mathcal{O}(\omega^2)$ and higher are associated with the polarizabilities of the dark-matter candidate.

Dispersive effects in light propagation are controlled by the group velocity v_g , so that the light emitted from a source a distance l away has an arrival time of $t(\omega) = l/v_g$. For very distant sources we must also take the cosmological expansion into account [22], so that as we look back to a light source at redshift z , we note that the dark-matter density accrues a scale factor of $(1+z)^3$, whereas the photon energy is blue shifted by a factor of $1+z$ relative to its present-day value ω_0 [22]. Thus the light arrival time $t(\omega_0, z)$ is

$$t(\omega_0, z) = \int_0^z \frac{dz'}{H(z')} \left(1 + \frac{\rho_0(1+z')^3}{4M^2} \left(\frac{-A_0}{((1+z')\omega_0)^2} + A_2 + 3A_4(1+z')^2\omega_0^2 + \mathcal{O}(\omega_0^4) \right) \right) \quad (1)$$

with the Hubble rate $H(z') = H_0\sqrt{(1+z')^3\Omega_M + \Omega_\Lambda}$. We employ the cosmological parameters determined through the combined analysis of WMAP five-year data in the Λ CDM

model with distance measurements from Type Ia supernovae (SN) and with baryon acoustic oscillation information from the distribution of galaxies [3]. Thus the Hubble constant today is $H_0 = 70.5 \pm 1.3 \text{ km s}^{-1} \text{ Mpc}^{-1}$, whereas the fraction of the energy density in matter relative to the critical density today is $\Omega_M = 0.274 \pm 0.015$ and the corresponding fraction of the energy density in the cosmological constant Λ is $\Omega_\Lambda = 0.726 \pm 0.015$ [3].

We find that the time delay is characterized by powers of ω^2 and unknown coefficients A_{2j} . Different strategies must be employed to determine them. The A_2 term incurs no frequency-dependent shift in the speed of light, so that to infer its presence one needs a distance measure independent of z , much as in the manner one infers a nonzero cosmological constant from Type Ia supernovae data. Interestingly, as $A_2 > 0$ it has the same phenomenological effect as a nonzero cosmological constant; the longer arrival time leads to an inferred larger distance scale. Cosmologically, though, its effect is very different as it scales with the dark-matter density; it acts as grey dust. The remaining terms can be constrained by comparing arrival times for differing observed ω_0 .

The determination of A_0 and A_4 require the analysis of the GRB light curves at extremely low and high energies, respectively, and probe disjoint dark-matter models. As a first application of our method, we use radio afterglow data to determine A_0 and thus to yield a direct limit on the electric-charge to mass of dark matter. This quantity gives insight into the mechanism of dark matter stability. If dark matter possesses an internal symmetry, e.g., it cannot decay to lighter particles and conserve its hidden charge. Such dynamics can also conspire to give dark matter a slight electric charge [23–25], which, no matter how small, reveals the existence of its hidden interactions and the reason for its stability.

To determine A_0 we consider GRBs with known redshift in which a radio afterglow is also detected. We collect the data and describe the criteria used in its selection in the supplementary material [26]. The time lag between the initial detection of the GRB at some energy and the detection of the radio afterglow is $\tau = t(\omega_0^{\text{low}}, z) - t(\omega_0^{\text{high}}, z)$. If we first observe the GRB at keV energies and compare with the observed arrival time in radio frequencies, then the terms in positive powers of ω_0 , as well as the term in $1/(\omega_0^{\text{high}})^2$, are negligible; we let $\omega \equiv \omega_0^{\text{low}}$. In order to assess reliable limits on A_0 we must separate propagation effects from intrinsic source effects. Statistically, we expect time delays intrinsic to the source to be independent of z , and the time delay from propagation to depend on z and ω in a definite way. Such notions have been previously employed in searches for Lorentz invariance violation [21]. We separate propagation and emission effects, respectively, via

$$\frac{\tau}{1+z} = \tilde{A}_0 \frac{K(z)}{\nu^2} + \delta((1+z)\nu) \quad (2)$$

where $K(z) \equiv (1+z)^{-1} \int_0^z dz' (1+z') H(z')^{-1}$ depends on the cosmological past through the Hubble rate $H(z)$ and $\delta((1+z)\nu)$ allows for a frequency-dependent time lag for emission from the GRB in the GRB rest frame. The frequency $\nu \equiv \omega/2\pi$, and \tilde{A}_0 contains the millicharge-to-mass ratio ε/M , i.e., $4\pi^2 \tilde{A}_0 = -A_0 \rho_0 / 4M^2 = 2\pi \alpha \varepsilon^2 \rho_0 / M^2$ with $\rho_0 \simeq 1.19 \times 10^{-6} \text{ GeV/cm}^3$ [3] and α the fine-structure constant. To provide a context, we first consider the value of $|\varepsilon|/M$ which would result were we to attribute the time lag associated with the radio afterglow of one GRB to a propagation effect. Choosing the GRB with the largest value of $K(z)/\nu^2$, we have a time lag of 2.700 ± 0.006 day associated with GRB 980703A at $z = 0.967 \pm 0.001$ measured at a frequency of 1.43 GHz. With Eq. (2), setting $\delta = 0$, and noting that $K(z)/\nu^2 = 1170 \pm 10 \text{ Mpc GHz}^{-2}$ if the errors in its inputs are uncorrelated, the measured time lag fixes $|\varepsilon|/M \simeq 9 \times 10^{-6} \text{ eV}^{-1}$. Since there are no known examples of

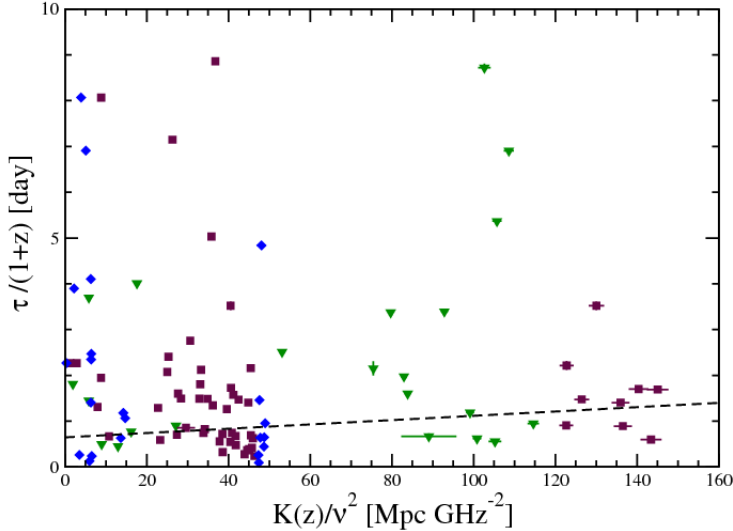


FIG. 1: The time lag τ determined from the observation of a GRB and its radio afterglow plotted as a function of $K(z)/\nu^2$ with $\nu = \omega/2\pi$, employing the data reported in the supplementary material [26]. The points correspond to frequency windows of 4.0 – 12 GHz (\blacktriangledown , green), 12 – 30 GHz (\blacksquare , maroon), and 30 – 75 GHz (\blacklozenge , blue) in the GRB rest frame. Points with $(1+z)\nu < 4.0$ GHz do not appear within the chosen frame of the figure. The fit of Eq. (2) to the data with $(1+z)\nu > 4.0$ GHz with a scale factor in the uncertainty in $\tau/(1+z)$ of 450, to compensate for environmental effects in the vicinity of the emission from the GRB, yields $\tilde{A}_0 = 0.0010 \pm 0.0019$ day $\text{Ghz}^2 \text{Mpc}^{-1}$ and $\delta = 0.65 \pm 0.10$ day with $\chi^2/\text{ndf} = 1.13$. Thus $\tilde{A}_0 < 0.005$ day $\text{Ghz}^2 \text{Mpc}^{-1}$ at 95% CL to yield $|\varepsilon|/M < 1 \times 10^{-5} \text{ eV}^{-1}$ at 95% CL. The statistical scale factors are not shown explicitly. For clarity of presentation we display time lags in the GRB rest frame of less than 10 days only.

a radio afterglow preceding a GRB, this single time lag in itself represents a conservative limit. Turning to our data sample of 53 GRBs, we plot the measured time lag versus $K(z)/\nu^2$ in Fig. 1 and make a least-squares fit of Eq. (2) to determine \tilde{A}_0 and $\delta((1+z)\nu)$. We require $\tilde{A}_0 > 0$ as demanded by our model. Fitting to the points with frequencies of 4.0 – 75 GHz in the GRB rest frame, we determine $|\varepsilon|/M < 1 \times 10^{-5} \text{ eV}^{-1}$ at 95% CL, which is comparable to our limit derived from a single observation of GRB 980703A. The dependence of our fit results on the selected frequency window, as well as the stability of our fits to the significance of the radio afterglow observation, to evolution effects in z , and to the more poorly determined red shifts and radio afterglows is discussed in the supplementary information [26].

We have found a direct observational limit on the dark-matter electric-charge-to-mass ratio. Our study probes for a charge imbalance averaged over cosmological distance scales, without regard to its sign, at distance scales shorter than the wavelengths of the radio observations in our data set. Our bound rules out the possibility of charged “Q-balls” [25, 27] of less than 100 keV in mass as dark-matter candidates. Our limit holds regardless of the manner in which the dark matter is produced, though we can compare it to limits arising

from the nonobservation of the effects of millicharged particle production. For example, for $M \sim 0.05$ eV, they are crudely comparable to the strongest bound from laboratory experiments [28, 29], for $|\varepsilon| < 3 - 4 \times 10^{-7}$ for $M \lesssim 0.05$ eV [29]. In comparison the model-independent bound arising from induced distortions in the cosmic microwave background (CMB) radiation is $|\varepsilon| \leq 10^{-7}$ for $M < 0.1$ eV, though model-dependent constraints reach $|\varepsilon| \leq 10^{-9}$ for $M < 2 \times 10^{-4}$ eV [30]. Cosmological limits also arise from observations of the Sunyaev-Zeldovich effect for which, e.g., $|\varepsilon| \leq 3 \times 10^{-7}$ for $M \sim 10^{-6}$ eV [31]. For these light masses our limit is stronger, which shows that millicharged particles of such mass and charge are not the primary constituents of dark matter. Limits also arise from stellar evolution and big-bang nucleosynthesis constraints, for which the strongest is $|\varepsilon| < 2 \times 10^{-14}$ for $M < 5$ keV [28], as well as from the manner in which numerical simulations of galactic structure confront observations [32–34]. We offer a visual summary of this discussion in Fig. 2. Indirect limits can be evaded: for example, in some models, the dynamics which gives rise to millicharged matter are not operative at stellar temperatures [29, 35]; other models evade the galactic structure constraints [25, 27].

Our limit also significantly restricts the phase space of models with hyperweak gauge interactions and millicharged particles which can arise in string theory scenarios [31, 36] as viable dark-matter candidates. We estimate that our limit can be improved considerably before the dispersive effects from ordinary charged matter become appreciable [37]. The largest such contribution to \tilde{A}_0 should come from free electrons. We estimate the cosmological free electron energy density ρ_e to be no larger than $\rho_e = (M_e/M_p)\rho_{\text{cr}}\Omega_b \approx 0.130$ eV/cm³ [3], where Ω_b is the fraction of the energy density in baryons with respect to the critical density today and M_e and M_p are the electron and proton mass, respectively. Replacing ρ_0 with ρ_e and ε/M with $1/M_e$ in \tilde{A}_0 we find that our limit would have to improve by $\mathcal{O}(2 \times 10^{-3})$ before the contribution from free electrons could be apparent. We set our limit of $|\varepsilon|/M < 1 \times 10^{-5}$ eV⁻¹ from existing radio observations at no less than 4 GHz in the GRB rest frame, so that our limit is certainly operative if $\omega_{\text{th}}/2\pi > 4$ GHz, or crudely, if $M > 8 \times 10^{-6}$ eV. Studies of the polarizability in QED [38], for which $\omega_{\text{th}} = 0$, also reveal the analytic structure in ω we have assumed for the forward Compton amplitude. Thus we believe our limit to be of broader validity, so that the lower limit on the mass can be less than 8×10^{-6} eV, though it is model dependent and set by the Lee-Weinberg constraint [39], much as the minimum mass of $\sim 6 \times 10^{-6}$ eV is determined in the axion model of Ref. [18]. Forward scattering is coherent irrespective of whether the photon wavelength is large compared to the interparticle spacing, so that we expect our results to persist in the dilute particle limit as well, as supported by laboratory studies [40]. One further comment: at a frequency of 4 GHz our limit implies that we probe the average net charge of dark matter, with no constraint on its sign, at length scales of no longer than 8 cm. Our limits can be significantly bettered through GRB radio afterglow studies at longer wavelengths.

We thank Keith Olive for an inspiring question and Scott Dodelson, Renée Fatemi, Wolfgang Korsch, and Tom Troland for helpful comments. SG would also like to thank Stan Brodsky for imparting an appreciation of the low-energy theorems in Compton scattering and the Institute for Nuclear Theory and the Center for Particle Astrophysics and Theoretical Physics at Fermilab for gracious hospitality. This work is supported, in part, by the

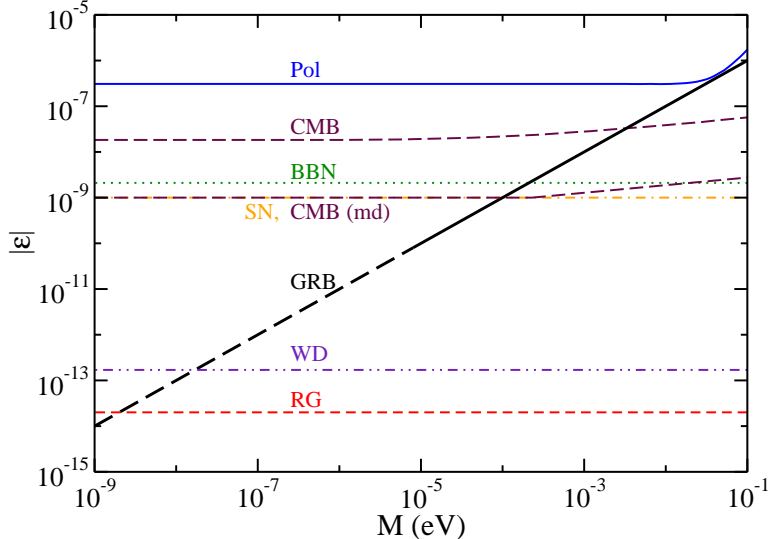


FIG. 2: Comparison of our direct limit on the absolute electric charge of dark matter, $|\varepsilon|$, in units of e with candidate mass M with limits from other sources stemming from millicharged particle production. Our limit derives from observations of GRBs and their radio afterglows and is marked “GRB” (solid, black), so that the region above that line is excluded. The condition $\omega < \omega_{\text{th}}$, as discussed in text, sets the lower endpoint of the solid line. Since Eq. (2) persists in QED, for which $\omega_{\text{th}} = 0$, we expect our limit to persist for lighter, cold dark matter as well, as indicated by the dashed line. The strongest laboratory limits, which are for fermions, are marked “Pol” (solid, blue) [29], and the strongest limits from induced distortions in the CMB, which are also for fermions, are marked “CMB” (long-dashed, maroon) — the upper curve is the model-independent limit, whereas the lower curve is the model-dependent (md) limit [30]. Constraints on $|\varepsilon|$ emerge from limits on novel energy-loss mechanisms in stars and supernovae; such limits also fail to act if $|\varepsilon|$ is too large. The limit from plasmon decay in red-giants is marked by “RG” (short-dashed, red) [28], the same limit in white dwarfs is marked by “WD” (dot-dot-dashed, indigo) [28], and the limit from SN 1987A is marked by “SN” (dot-dashed, orange) [28]. The RG limit acts if $|\varepsilon| \lesssim 10^{-8}$ [28]. We have also reported the limit from big-bang nucleosynthesis, marked by “BBN” (dotted, green), from Ref. [28] as well.

U.S. Department of Energy under contract DE-FG02-96ER40989.

-
- [1] D. N. Spergel *et al.* [WMAP Collaboration], *Astrophys. J. Suppl.* **148**, 175 (2003).
 - [2] M. Tegmark *et al.* [SDSS Collaboration], *Phys. Rev. D* **69**, 103501 (2004).
 - [3] E. Komatsu *et al.* [WMAP Collaboration], *Astrophys. J. Suppl.* **180**, 330 (2009).
 - [4] S. Gardner, *Phys. Rev. Lett.* **100**, 041303 (2008).
 - [5] P. Ullio, L. Bergstrom, J. Edsjo, and C. G. Lacey, *Phys. Rev. D* **66**, 123502 (2002).
 - [6] J. L. Hall, in *Atomic Masses and Fundamental Constants*, edited by J. H. Sanders and A. H. Wapstra (Plenum, New York, 1976), p. 322.
 - [7] B. Warner and R. Nather, *Nature* **222**, 157 (1969).
 - [8] B. E. Schaefer, *Phys. Rev. Lett.* **82**, 4964 (1999).

- [9] G. Amelino-Camelia *et al.*, *Nature* **393**, 763 (1998).
- [10] A. A. Abdo *et al.* [Fermi LAT Collaboration], *Nature* **462**, 331 (2009).
- [11] M. Gell-Mann, M. L. Goldberger, and W. E. Thirring, *Phys. Rev.* **95**, 1612 (1954).
- [12] M. L. Goldberger, *Phys. Rev.* **97**, 508 (1955).
- [13] T. R. Hemmert, B. R. Holstein, J. Kambor, and G. Knöchlein, *Phys. Rev. D* **57**, 5746 (1998).
- [14] W. E. Thirring, *Philos. Mag.* **41**, 1193 (1950).
- [15] E. Fermi, *Nuclear Physics, Revised Edition* (University of Chicago Press, Chicago, IL, 1974), p. 202.
- [16] R. G. Newton, *Scattering Theory of Waves and Particles, 1st Edition* (McGraw-Hill, New York, 1966), p. 24ff.
- [17] M. E. Peskin and D. V. Schroeder, *An Introduction to Quantum Field Theory* (Addison-Wesley Publishing Company, Reading, MA, 1995).
- [18] P. Sikivie and Q. Yang, *Phys. Rev. Lett.* **103**, 111301 (2009).
- [19] L. I. Lapidus and Chou Kuang-Chao, *J. Exptl. Theoret. Phys. (USSR)* **39**, 1286 (1960) [*Sov. Phys. JETP* **12**, 898 (1961)].
- [20] S. J. Brodsky and J. R. Primack, *Ann. Phys.* **52**, 315 (1969).
- [21] J. R. Ellis *et al.*, *Astrophys. J.* **535**, 139 (2000).
- [22] U. Jacob and T. Piran, *JCAP* **0801**, 031 (2008).
- [23] B. Holdom, *Phys. Lett. B* **166**, 196 (1986).
- [24] D. Feldman, Z. Liu, and P. Nath, *Phys. Rev. D* **75**, 115001 (2007).
- [25] A. Kusenko and P. J. Steinhardt, *Phys. Rev. Lett.* **87**, 141301 (2001).
- [26] See appended supplementary information.
- [27] I. M. Shoemaker and A. Kusenko, *Phys. Rev. D* **78**, 075014 (2008).
- [28] S. Davidson, S. Hannestad, and G. Raffelt, *JHEP* **0005**, 003 (2000).
- [29] M. Ahlers *et al.*, *Phys. Rev. D* **77**, 095001 (2008).
- [30] A. Melchiorri, A. Polosa, and A. Strumia, *Phys. Lett. B* **650**, 416 (2007).
- [31] C. Burrage, J. Jaeckel, J. Redondo, and A. Ringwald, *JCAP* **11**, 002 (2009).
- [32] B. A. Gradwohl and J. A. Frieman, *Astrophys. J.* **398**, 407 (1992).
- [33] L. Ackerman, M. R. Buckley, S. M. Carroll, and M. Kamionkowski, *Phys. Rev. D* **79**, 023519 (2009).
- [34] J. L. Feng, M. Kaplinghat, H. Tu, and H. B. Yu, *JCAP* **07**, 004 (2009).
- [35] E. Massó and J. Redondo, *Phys. Rev. Lett.* **97**, 151802 (2006).
- [36] C. P. Burgess *et al.*, *JHEP* **07**, 073 (2008).
- [37] L. Bombelli and O. Winkler, *Class. Quant. Grav.* **21**, L89 (2004).
- [38] E. Llanta and R. Tarrach, *Phys. Lett. B* **78**, 586 (1978).
- [39] B. W. Lee and S. Weinberg, *Phys. Rev. Lett.* **39**, 165 (1977).
- [40] G. K. Campbell *et al.*, *Phys. Rev. Lett.* **94**, 170403 (2005).

Supplementary Information

I. GAMMA-RAY BURST DATA

From the publicly available data, we consider the gamma-ray bursts (GRB) with known redshifts and detected radio afterglows through March, 2009. Tables 1–4 collect the GRBs with these properties which satisfy certain criteria. We demand that the energy of the initially detected gamma-ray burst in its rest frame be compatible with the energy range of the Fermi Gamma-Burst Monitor. This excludes the X-ray flashes GRB 080109A and GRB 020903A. To determine whether an observation of the radio flux is indeed a detected radio afterglow, we demand that the radio flux detection be within the error box of the location of the observed GRB, that it not be a site of previously observed radio activity, and that it be significantly non-zero. We use the criterion employed by Ref. [55] and thus require that the radio observation be nonzero by three standard deviations or more to be termed a detection. Such considerations exclude GRB 030277A, GRB 980425A, and GRB 011130A. Consequently, we find 53 GRBs to consider, for which we report all detected radio frequencies of 75 GHz or less. We report the time of the initial detection of the GRB and the time of the detection of a particular observation frequency ν in the associated radio afterglow (RA). We calculate the time lag between the detection of a particular radio frequency and the initial detection of the GRB from these quantities.

Remarks concerning the collected data are in order. A redshift marked with an asterisk * means that no certainty has been reported in the work which determines it. In those cases, we assume the uncertainty in the redshift to be plus or minus one unit in the last significant figure reported. The redshift we report for GRB 021004A is the average of those reported in Refs. [145, 146]. For the redshifts marked with a circle $^{\circ}$, the associated publication states that the reported redshift is either a lower limit or the “likely” value. In the particular case of GRB 970508A, work in refinement of the upper bound on the red shift has been reported in Ref. [204]. For the frequency marked with a double dagger ‡ , observations were made in the frequency range from 14.5 GHz to 17.5 GHz.

We also note which radio detections have lesser significance, so that detections with a significance between 3σ and 4σ are marked with a sharp $^{\sharp}$, whereas detections with a significance between 4σ and 5σ are marked with a flat $^{\flat}$. For time lags marked with a dagger † , we assume the uncertainty in the time lag to be plus or minus one unit in the last significant figure of the reported detection time of a particular radio frequency. If a radio frequency detection reports an observation time interval, the time lag is calculated from the midpoint of the time interval, and we take one half of the observation time as the uncertainty in the time lag. The RA time reported in these cases is that of the midpoint of the observation time.

To realize the limits reported in the main body of our paper, we fit to Eq. (2) of that source. We find that large statistical scale factors must be employed to realize good fits to the data. This may stem, in part, from the circumburst environment, and, more generally, from time delay effects which arise from neither source effects nor propagation effects across the expanse of space. The nature of the circumburst environment of GRB 050904A is discussed in Ref. [111].

To study how our limits rely on the details of our data set, we compare fits with frequency in the source rest frame. We also study how the fits change with the significance of the included

radio observations, with omitting radio observations with reported integration times, and with omitting more poorly determined red shifts. We also try to study source evolution effects with z . As to the frequency dependence, differences do emerge if we include points at the observed frequency of 1.43 GHz. This portion of the data set admits time delays in the GRB rest frame of a month and more, and larger scale factors are required to yield fits of comparable quality. Fitting data satisfying $(1+z)\nu > 4.0$ GHz, for which with a scale factor of 450 applied to the error in $\tau/(1+z)$ we find $\chi^2/\text{ndf} = 1.13$ with $\tilde{A}_0 = 0.0010 \pm 0.002$ day Ghz² Mpc⁻¹ and $\delta((1+z)\nu) = 0.65 \pm 0.10$ day, or $\tilde{A}_0 < 0.005$ day Ghz² Mpc⁻¹ at 95% CL. Were we to fit all the data points we would require a scale factor of 685 to yield a fit of $\chi^2/\text{ndf} = 1.13$ from which we would find $\tilde{A}_0 < 0.007$ day Ghz² Mpc⁻¹ at 95% CL. We thus restrict our discussion henceforth to the portion of the data set which satisfies $(1+z)\nu > 4.0$ GHz. If we now restrict our fit to points in which the significance of the radio observation is 5σ or more, then our limit on the slope is still $\tilde{A}_0 < 0.005$ day Ghz² Mpc⁻¹ at 95% CL, though we must increase the scale factor to 512 to recover a fit of comparable quality. Some of the RA measurements have reported integration times and hence determinable uncertainties, whereas others do not. Repeating the fits without the points with reported integration times yields no significant difference in the fit, though we must increase the scale factor to 467 to yield a fit of comparable quality. This may well follow as the dropped points do have larger errors and hence play a lesser role in the original fit. If we now return to our original data set and omit those points for which the determined redshift is a lower limit or merely “likely,” the limits do weaken. For example, with a scale factor of 419, we find $\chi^2/\text{ndf} = 1.13$ with $\tilde{A}_0 = 0.0053 \pm 0.0048$ day Ghz² Mpc⁻¹ and $\delta((1+z)\nu) = 0.41 \pm 0.21$, so that the limit on the slope at 95% CL is roughly a factor of 3 worse. This can be rationalized as these poorly known redshifts possess large z . Finally, to study the effects of cosmological evolution on the GRBs, we repeat our fit with $z > 1$ and find similar results. That is, for a scale factor of 539 we determine $\chi^2/\text{ndf} = 1.14$ with $\tilde{A}_0 = 0.0017 \pm 0.0023$ day Ghz² Mpc⁻¹ and $\delta((1+z)\nu) = 0.58 \pm 0.12$, to yield $\tilde{A}_0 < 0.006$ day Ghz² Mpc⁻¹ at 95% CL. Thus the effects of cosmological evolution appear to be small.

GRB	Redshift	GRB Time (UT)	RA Time (UT)	Frequency (GHz)	Time Lag (d)
090328A	$0.736 \pm 0.001^*$ [41]	09:36:46 [42]	Mar 30.99 [43]	8.46	$2.59 \pm 0.01^\dagger$
090323A	$3.6 \pm 0.1^*$ [44]	00:02:42.63 [45]	Mar 27.38 [46]	8.46	$4.38 \pm 0.01^\dagger$
090313A	$3.375 \pm 0.001^*$ [47]	09:06:27 [48]	Mar 16.13 [49]	16^\ddagger	2.75 ± 0.05
081007A	0.5295 ± 0.0001 [50]	05:23:52 [51]	Oct 09.19 [52]	8.46	$1.97 \pm 0.01^\dagger$
080810A	$3.35 \pm 0.01^*$ [53]	13:10:12 [54]	Aug 13.36 [55]	$8.46^\#$	$2.81 \pm 0.01^\dagger$
080603A	$1.6880 \pm 0.0001^*$ [56]	11:18:11 [57]	Jun 07.42 [58]	8.46	$3.95 \pm 0.01^\dagger$
080319B	$0.937 \pm 0.001^*$ [59]	06:12:47 [60]	Mar 21.56 [61]	4.86^b	$2.30 \pm 0.01^\dagger$
071122A	$1.14 \pm 0.01^*$ [62]	01:23:25 [63]	Nov 24.94 [64]	8.46	$2.8779 \pm 0.0001^\dagger$
071020A	$2.145 \pm 0.001^{*\circ}$ [65]	07:02:26 [66]	Oct 22.4671 [67]	8.46	$2.1737 \pm 0.0004^\dagger$
071010B	$0.947 \pm 0.001^*$ [68]	20:45:47 [69]	Oct 13.7675 [70]	8.46	$2.9024 \pm 0.0004^\dagger$
071003A	$1.60435 \pm 0.00001^*$ [71]	07:40:55 [72]	Oct 05.0771 [73]	8.46	$1.7570 \pm 0.0004^\dagger$
071003A			Oct 07.16 [74]	4.86^b	$3.84 \pm 0.01^\dagger$
070612A	$0.617 \pm 0.001^*$ [75]	02:38:41 [76]	Jun 15.59 [77]	$4.9^\#$	3.48 ± 0.25
070612A			Jun 16.00 [74]	8.46	$3.89 \pm 0.01^\dagger$
070125A	$1.547 \pm 0.001^{*\circ}$ [78]	07:20:42 [79]	Jan 29.32 [74]	8.46	$4.01 \pm 0.01^\dagger$
070125A			Jan 30.95 [80]	$4.9^\#$	5.64 ± 0.25
061121A	$1.314 \pm 0.001^*$ [81]	15:22:29 [82]	Nov 22.3825 [83]	8.46	$0.7419 \pm 0.0004^\dagger$
060418A	1.4901 ± 0.0001 [84]	03:06:08 [85]	Apr 22.43 [86]	8.46^b	$4.30 \pm 0.01^\dagger$
060218A	$0.0331 \pm 0.0001^*$ [87]	03:34:30 [88]	Feb 20.02 [89]	8.46	$1.87 \pm 0.01^\dagger$
060218A			Feb 21.97 [89]	4.86	$3.82 \pm 0.01^\dagger$
060116A	6.6 ± 0.15 [90]	08:37:27 [91]	Jan 21.21 [92]	$8.46^\#$	$4.85 \pm 0.01^\dagger$
051221A	$0.5465 \pm 0.0001^*$ [93]	01:51:12.976 [94]	Dec 21.99 [95]	8.46	$0.91 \pm 0.01^\dagger$
051111A	$1.55 \pm 0.01^*$ [96]	05:59:39 [97]	Nov 13.15 [98]	$8.5^\#$	$1.90 \pm 0.01^\dagger$
051109A	$2.346 \pm 0.001^*$ [99]	01:12:20 [100]	Nov 11.15 [101]	8.5^b	$2.10 \pm 0.01^\dagger$
051022A	$0.8 \pm 0.1^*$ [102],[103]	13:07:58 [104]	Oct 23.7 [103]	4.9	1.2 ± 0.1
051022A			Oct 24.09 [105]	8.5	$1.54 \pm 0.01^\dagger$
050922C	$2.199 \pm 0.001^{*\circ}$ [106]	19:55:54.480 [107]	Sep 24.17 [108]	$8.46^\#$	$1.34 \pm 0.01^\dagger$
050904A	6.29 ± 0.01 [109]	01:51:44 [110]	Oct 09.34 [111]	8.46	$35.26 \pm 0.01^\dagger$
050820A	$2.6147 \pm 0.0001^*$ [112]	06:34:53 [113]	Aug 21.20 [114]	8.46	$0.93 \pm 0.01^\dagger$
050820A			Aug 22.42 [74]	$4.86^\#$	$2.15 \pm 0.01^\dagger$

TABLE I: Gamma ray burst and radio afterglow data from mid-2005 through March, 2009.

GRB	Redshift	GRB Time (UT)	RA Time (UT)	Frequency (GHz)	Time Lag (d)
050730A	$3.97 \pm 0.01^*$ [115]	19:58:23 [116]	Aug 02.03 [117]	8.5	$2.20 \pm 0.01^\dagger$
050724A	0.258 ± 0.002 [118]	12:34:09 [119]	Jul 25.09 [120]	8.46	$0.57 \pm 0.01^\dagger$
050603A	$2.821 \pm 0.001^*$ [121]	06:29:00.767 [122]	Jun 03.62 [123]	8.5	$0.35 \pm 0.01^\dagger$
050603A			Jun 09.73 [74]	4.86 ^b	$6.46 \pm 0.01^\dagger$
050525A	$0.606 \pm 0.001^*$ [124]	00:02:53 [125]	May 25.42 [126]	22.5	$0.42 \pm 0.01^\dagger$
050525A			May 27.10 [74]	15 [‡]	$2.10 \pm 0.01^\dagger$
050525A			May 28.33 [74]	8.46 [‡]	$3.33 \pm 0.01^\dagger$
050416A	0.6535 ± 0.0002 [127]	11:04:44.5 [128]	Apr 22.04 [129]	4.86 ^b	$5.58 \pm 0.01^\dagger$
050416A			Apr 28.28 [74]	8.46 ^b	$11.82 \pm 0.01^\dagger$
050401A	$2.9 \pm 0.01^*$ [130]	14:20:11 [131]	Apr 07.29 [132]	8.5 [‡]	$5.69 \pm 0.01^\dagger$
050315A	$1.949 \pm 0.001^*$ [133]	20:59:42 [134]	Mar 16.68 [135]	8.5 ^b	$0.81 \pm 0.01^\dagger$
031203A	$0.105 \pm 0.001^*$ [136], [137]	22:01:28 [138]	Dec 05.52 [137]	8.46	$1.60 \pm 0.01^\dagger$
031203A			Dec 08.35 [137]	4.86	$4.43 \pm 0.01^\dagger$
031203A			Dec 17.38 [137]	22.5	$13.46 \pm 0.01^\dagger$
031203A			Jan 12.29 [137]	1.43	$39.37 \pm 0.01^\dagger$
030329A	$0.1687 \pm 0.0001^*$ [139]	11:36:58 [140]	Mar 30.06 [141]	8.46	$0.58 \pm 0.01^\dagger$
030329A			Mar 30.53 [141]	4.86 ^b	$1.05 \pm 0.01^\dagger$
030329A			Apr 01.13 [141]	15	$2.65 \pm 0.01^\dagger$
030329A			Apr 01.13 [141]	22.5	$2.65 \pm 0.01^\dagger$
030329A			Apr 01.13 [141]	43.3	$2.65 \pm 0.01^\dagger$
030329A			Jun 04.01 [141]	1.43	$66.53 \pm 0.01^\dagger$
030226A	$1.986 \pm 0.001^\circ$ [142]	03:46:31.99 [143]	Feb 27.25 [144]	8.46	$1.09 \pm 0.01^\dagger$
030226A			Mar 10.41 [144]	22.5 ^b	$12.25 \pm 0.01^\dagger$
021004A	2.331 ± 0.004 [145], [146]	12:06:13.57 [147]	Oct 05.29 [148]	22.5	$0.79 \pm 0.01^\dagger$
021004A			Oct 05.29 [74]	8.46 ^b	$0.79 \pm 0.01^\dagger$
021004A			Oct 08.04 [149]	15 [‡]	3.54 ± 0.08
021004A			Oct 10.17 [150]	4.86	$5.67 \pm 0.01^\dagger$
020813A	$1.2545 \pm 0.0001^*$ [151]	02:44:19.17 [152]	Aug 14.36 [153], [154]	8.46	$1.25 \pm 0.01^\dagger$
020813A			Aug 15.25 [154]	4.86	$2.14 \pm 0.01^\dagger$

TABLE II: Gamma ray burst and radio afterglow data from mid-2002 through mid-2005.

GRB	Redshift	GRB Time (UT)	RA Time (UT)	Frequency (GHz)	Time Lag (d)
020405A	0.695 ± 0.005 [155]	00:41:26 [156]	Apr 06.22 [157]	8.46	$1.19 \pm 0.01^\dagger$
020405A			Apr 08.38 [74]	4.86 [#]	$3.35 \pm 0.01^\dagger$
011211A	$2.142 \pm 0.001^*$ [158]	19:09:21 [159]	Dec 18.58 [160]	8.46	$6.78 \pm 0.01^\dagger$
011211A			Dec 19.56 [160]	22.5 [#]	$7.76 \pm 0.01^\dagger$
011121A	0.362 ± 0.001 [161]	18:47:21 [162]	Nov 22.83 [163]	8.70	$1.05 \pm 0.01^\dagger$
011121A			Nov 25.20 [163]	4.80 [#]	$3.42 \pm 0.01^\dagger$
010921A	0.450 ± 0.005 [164]	05:15:50.56 [165]	Oct 17.15 [166]	4.86	$25.93 \pm 0.01^\dagger$
010921A			Oct 17.15 [166]	8.46	$25.93 \pm 0.01^\dagger$
010921A			Oct 17.15 [166]	22.5 [#]	$25.93 \pm 0.01^\dagger$
010222A	$1.477 \pm 0.001^*$ [167]	07:23:30 [168]	Feb 22.62 [169]	22 ^b	$0.31 \pm 0.01^\dagger$
010222A			Feb 23.66 [170]	8.46	$1.35 \pm 0.01^\dagger$
010222A			Feb 24.56 [170]	4.86 [#]	$2.25 \pm 0.01^\dagger$
000926A	$2.066 \pm 0.001^{*\circ}$ [171]	23:49:33 [172]	Sep 28.17 [173]	8.46	$1.18 \pm 0.01^\dagger$
000926A			Sep 29.726 [173]	4.86	$2.733 \pm 0.001^\dagger$
000926A			Oct 04.186 [173]	22.5	$7.193 \pm 0.001^\dagger$
000911A	1.0585 ± 0.0001 [174]	07:15:25 [175]	Sep 14.36 [174]	8.46	$3.06 \pm 0.01^\dagger$
000911A			Sep 22.35 [174]	4.86 [#]	$11.05 \pm 0.01^\dagger$
000418A	1.1181 ± 0.0001 [176]	09:53:10 [177]	Apr 29.07 [178]	8.46	$10.66 \pm 0.01^\dagger$
000418A			May 03.04 [178]	4.86	$14.63 \pm 0.01^\dagger$
000418A			May 03.04 [178]	22.46	$14.63 \pm 0.01^\dagger$
000418A			May 07.18 [178]	8.35	$18.77 \pm 0.01^\dagger$
000301C	2.0335 ± 0.0003 [179]	09:51:37 [180]	Mar 04.98 [181]	15.0 ^b	$3.57 \pm 0.01^\dagger$
000301C			Mar 05.67 [181]	4.86 ^b	$4.26 \pm 0.01^\dagger$
000301C			Mar 05.67 [181]	8.46	$4.26 \pm 0.01^\dagger$
000301C			Mar 05.67 [181]	22.5 ^b	$4.26 \pm 0.01^\dagger$
991216A	1.00 ± 0.02 [182]	16:07:01 [183]	Dec 17.783 [184]	4.8	1.11 ± 0.13
991216A			Dec 18.00 [185]	15 ^b	$1.33 \pm 0.01^\dagger$
991216A			Dec 18.16 [185]	8.46	$1.49 \pm 0.01^\dagger$
991216A			Dec 18.32 [185]	8.42	$1.65 \pm 0.01^\dagger$
991216A			Jan 03.11 [185]	4.86 ^b	$17.44 \pm 0.01^\dagger$

TABLE III: Gamma ray burst and radio afterglow data from mid-1999 through mid-2002.

GRB	Redshift	GRB Time (UT)	RA Time (UT)	Frequency (GHz)	Time Lag (d)
991208A	0.707 ± 0.002 [186]	04:36:52 [187]	Dec 10.92 [188]	4.86	$2.73 \pm 0.01^\dagger$
991208A			Dec 10.92 [188]	8.46	$2.73 \pm 0.01^\dagger$
991208A			Dec 11.51 [188]	15.0	$3.32 \pm 0.01^\dagger$
991208A			Dec 14.84 [188]	30 [#]	$6.65 \pm 0.01^\dagger$
991208A			Dec 15.90 [188]	1.43 ^p	$7.71 \pm 0.01^\dagger$
991208A			Dec 21.96 [188]	14.97	$13.77 \pm 0.01^\dagger$
991208A			Dec 21.96 [188]	22.49	$13.77 \pm 0.01^\dagger$
990510A	$1.619 \pm 0.002^\circ$ [189]	08:49 [190]	May 13.68 [189]	8.7	3.31 ± 0.19
990510A			May 19.59 [189]	4.8 ^p	9.22 ± 0.24
990510A			May 19.59 [189]	8.6 ^p	9.22 ± 0.24
990506A	1.30658 ± 0.00004 [176]	11:23:31.0 [191]	May 08.13 [192]	8.46	$1.66 \pm 0.01^\dagger$
990123A	$1.61 \pm 0.01^*$ [193]	09:46:56.1 [194]	Jan 24.65 [195],[196]	8.46	$1.24 \pm 0.01^\dagger$
980703A	$0.967 \pm 0.001^*$ [197]	04:22:45 [198]	Jul 04.40 [199]	4.86	$1.22 \pm 0.01^\dagger$
980703A			Jul 07.35 [199]	8.46	$4.17 \pm 0.01^\dagger$
980703A			Jul 08.49 [199]	1.43 [#]	$5.31 \pm 0.01^\dagger$
970828A	0.9578 ± 0.0001 [200]	17:44:36 [201]	Sep 01.27 [200]	8.46 ^p	$3.53 \pm 0.01^\dagger$
970508A	$0.835 \pm 0.001^{*\circ}$ [202],[203],[204]	21:42 [205]	May 13.96 [206]	8.46	$5.06 \pm 0.01^\dagger$
970508A			May 15.09 [206]	1.43 [#]	$6.19 \pm 0.01^\dagger$
970508A			May 15.13 [206]	4.86	$6.23 \pm 0.01^\dagger$

TABLE IV: Gamma ray burst and radio afterglow data from 1997 through mid-1999.

II. REFERENCES

- [41] Cenko, S. B. *et al.* GRB 090328: Gemini South redshift. *GCN Circular* 9053, <http://gcn.gsfc.nasa.gov/gcn3/9053.gcn3> (2009).
- [42] McEnery, J. *et al.* Fermi LAT and GBM detections of GRB 090328. *GCN Circular* 9044, <http://gcn.gsfc.nasa.gov/gcn3/9044.gcn3> (2009).
- [43] Frail, D. A. *et al.* GRB 090328: Radio afterglow detection. *GCN Circular* 9060, <http://gcn.gsfc.nasa.gov/gcn3/9060.gcn3> (2009).
- [44] Chornock, R. *et al.* GRB 090323 Gemini-South redshift. *GCN Circular* 9028, <http://gcn.gsfc.nasa.gov/gcn3/9028.gcn3> (2009).
- [45] Ohno, M. *et al.* Fermi GBM and LAT detections of GRB 090323. *GCN Circular* 9021, <http://gcn.gsfc.nasa.gov/gcn3/9021.gcn3> (2009).
- [46] Harrison, F., Cenko, B., Frail, D. A., Chandra, P. & Kulkarni, S. GRB 090323: Radio afterglow detection. *GCN Circular* 9043, <http://gcn.gsfc.nasa.gov/gcn3/9043.gcn3> (2009).
- [47] Chornock, R. *et al.* GRB 090313: Gemini-S redshift. *GCN Circular* 8994, <http://gcn.gsfc.nasa.gov/gcn3/8994.gcn3> (2009).
- [48] Mao, J. *et al.* GRB 090313: Swift detection of a burst. *GCN Circular* 8980, <http://gcn.gsfc.nasa.gov/gcn3/8980.gcn3> (2009).
- [49] Pooley, G. *et al.* Radio detection of GRB 090313. *GCN Circular* 9003, <http://gcn.gsfc.nasa.gov/gcn3/9003.gcn3> (2009).
- [50] Berger, E. *et al.* GRB 081007: Gemini-south redshift. *GCN Circular* 8335, <http://gcn.gsfc.nasa.gov/gcn3/8335.gcn3> (2008).
- [51] Baumgartner, W. H. *et al.* GRB 081007: Swift detection of a burst with optical afterglow. *GCN Circular* 8330, <http://gcn.gsfc.nasa.gov/gcn3/8330.gcn3> (2008).
- [52] Soderberg, A. *et al.* GRB 081007: Radio detection. *GCN Circular* 8354, <http://gcn.gsfc.nasa.gov/gcn3/8354.gcn3> (2008).
- [53] Prochaska, J. X. *et al.* GRB 080810: Keck/HIRES spectroscopy. *GCN Circular* 8083, <http://gcn.gsfc.nasa.gov/gcn3/8083.gcn3> (2008).
- [54] Page, K. L. *et al.* GRB 080810: Swift detection of a burst with a bright optical afterglow. *GCN Circular* 8080, <http://gcn.gsfc.nasa.gov/gcn3/8080.gcn3> (2008).
- [55] Chandra, P. *et al.* Radio detection of GRB 080810 with the VLA. *GCN Circular* 8103, <http://gcn.gsfc.nasa.gov/gcn3/8103.gcn3> (2008).
- [56] Perley, D. A. *et al.* GRB 080603: Gemini-North redshift. *GCN Circular* 7791, <http://gcn.gsfc.nasa.gov/gcn3/7791.gcn3> (2008).
- [57] Paizis, A. *et al.* GRB 080603: A long GRB detected by INTEGRAL. *GCN Circular* 7790, <http://gcn.gsfc.nasa.gov/gcn3/7790.gcn3> (2008).
- [58] Chandra, P. *et al.* VLA detection of INTEGRAL burst GRB 080603A. *GCN Circular* 7855, <http://gcn.gsfc.nasa.gov/gcn3/7855.gcn3> (2008).
- [59] Vreeswijk, P. M. *et al.* VLT/UVES redshift of GRB 080319B from FeII fine-structure lines. *GCN Circular* 7451, <http://gcn.gsfc.nasa.gov/gcn3/7451.gcn3> (2008).
- [60] Beckmann, V. *et al.* GRB 080319A/B/C: INTEGRAL SPI-ACS light curves available. *GCN Circular* 7450, <http://gcn.gsfc.nasa.gov/gcn3/7450.gcn3> (2008).
- [61] Soderberg, A. *et al.* Radio detection of GRB 080319B. *GCN Circular* 7506, <http://gcn.gsfc.nasa.gov/gcn3/7506.gcn3> (2008).
- [62] Cucchiara, A. *et al.* GRB 071122: Gemini absorption redshift. *GCN Circular* 7124, <http://gcn.gsfc.nasa.gov/gcn3/7124.gcn3> (2007).

- [63] Stamatikos, M. *et al.* GRB 071122: Swift detection of a burst. *GCN Circular* 7121, <http://gcn.gsfc.nasa.gov/gcn3/7121.gcn3> (2007).
- [64] Chandra, P. *et al.* VLA radio detection of GRB 071122. *GCN Circular* 7132, <http://gcn.gsfc.nasa.gov/gcn3/7132.gcn3> (2007).
- [65] Jakobsson, P. *et al.* GRB 071020: VLT spectroscopy. *GCN Circular* 6952, <http://gcn.gsfc.nasa.gov/gcn3/6952.gcn3> (2007).
- [66] Holland, S. T. *et al.* GRB 071020: Swift detection of a bright burst. *GCN Circular* 6949, <http://gcn.gsfc.nasa.gov/gcn3/6949.gcn3> (2007).
- [67] Chandra, P. *et al.* Radio detection of GRB 071020 with the VLA. *GCN Circular* 6978, <http://gcn.gsfc.nasa.gov/gcn3/6978.gcn3> (2007).
- [68] Stern, D. *et al.* GRB 071010B: Keck/DEIMOS emission-line redshift. *GCN Circular* 6928, <http://gcn.gsfc.nasa.gov/gcn3/6928.gcn3> (2007).
- [69] Markwardt, C. B. *et al.* GRB 071010B: Swift detection of a burst. *GCN Circular* 6871, <http://gcn.gsfc.nasa.gov/gcn3/6871.gcn3> (2007).
- [70] Chandra, P. *et al.* VLA detection of radio afterglow of GRB 071010B. *GCN Circular* 6915, <http://gcn.gsfc.nasa.gov/gcn3/6915.gcn3> (2007).
- [71] Perley, D. A. *et al.* GRB 071003: Broadband follow-up observations of a very bright gamma-ray burst in a galactic halo. *Astrophys. J.* **688**, 470-490 (2008).
- [72] Schady, P. *et al.* GRB 071003: Swift detection of a bright burst. *GCN Circular* 6837, <http://gcn.gsfc.nasa.gov/gcn3/6837.gcn3> (2007).
- [73] Chandra, P. *et al.* Radio detection of GRB 071003 with the VLA. *GCN Circular* 6853, <http://gcn.gsfc.nasa.gov/gcn3/6853.gcn3> (2007).
- [74] Frail, D. Radio afterglow data. http://www.aoc.nrao.edu/~dfraill/radio_data_2002_new.dat (2002).
- [75] Cenko, S. B. *et al.* GRB 070612A: Gemini spectroscopic redshift. *GCN Circular* 6556, <http://gcn.gsfc.nasa.gov/gcn3/6556.gcn3> (2007).
- [76] Uehara, T. *et al.* GRB 070612A: Suzaku/WAM observation of the prompt emission. *GCN Circular* 6533, <http://gcn.gsfc.nasa.gov/gcn3/6533.gcn3> (2007).
- [77] v. d. Horst, A. J. *et al.* GRB 070612A: Possible WSRT radio detection. *GCN Circular* 6549, <http://gcn.gsfc.nasa.gov/gcn3/6549.gcn3> (2007).
- [78] Fox, D. B. *et al.* GRB 070125: Redshift $z \gtrsim 1.54$ from Gemini afterglow spectrum. *GCN Circular* 6071, <http://gcn.gsfc.nasa.gov/gcn3/6071.gcn3> (2007).
- [79] Bellm, E. *et al.* RHESSI Spectrum of GRB 070125. *GCN Circular* 6025, <http://gcn.gsfc.nasa.gov/gcn3/6025.gcn3> (2007).
- [80] v. d. Horst, A. J. *et al.* GRB 070125: WSRT radio detection. *GCN Circular* 6063, <http://gcn.gsfc.nasa.gov/gcn3/6063.gcn3> (2007).
- [81] Bloom, J. S., Perley, D. A. & Chen, H. W. GRB 061121: Spectroscopic redshift. *GCN Circular* 5826, <http://gcn.gsfc.nasa.gov/gcn3/5826.gcn3> (2006).
- [82] Page, K. L. *et al.* GRB 061121: Swift detection of a bright burst with an optical counterpart. *GCN Circular* 5823, <http://gcn.gsfc.nasa.gov/gcn3/5823.gcn3> (2006).
- [83] Chandra, P. *et al.* Radio detection of GRB 061121. *GCN Circular* 5843, <http://gcn.gsfc.nasa.gov/gcn3/5843.gcn3> (2006).
- [84] Prochaska, J. X. *et al.* GRB 060418: Further analysis of MIKE spectroscopy. *GCN Circular* 5002, <http://gcn.gsfc.nasa.gov/gcn3/5002.gcn3> (2006).
- [85] Falcone, A. D. *et al.* GRB 060418: Swift detection of a burst with bright x-ray and optical afterglow. *GCN Circular* 4966, <http://gcn.gsfc.nasa.gov/gcn3/4966.gcn3> (2006).

- [86] Frail, D. GRB 060418 data. <http://www.aoc.nrao.edu/~dfrail/grb060418.dat> (2006).
- [87] Mirabal, N. *et al.* GRB 060218: MDM redshift. *GCN Circular* 4792, <http://gcn.gsfc.nasa.gov/gcn3/4792.gcn3> (2006).
- [88] Cusumano, G. *et al.* GRB 060218: Swift-BAT detection of a possible burst. *GCN Circular* 4775, <http://gcn.gsfc.nasa.gov/gcn3/4775.gcn3> (2006).
- [89] Soderberg, A. M. *et al.* Relativistic ejecta from X-ray flash XRF 060218 and the rate of cosmic explosions. *Nature* **442**, 1014–1017 (2006).
- [90] Grazian, A. *et al.* GRB 060116: photometric redshift - the farthest GRB? *GCN Circular* 4545, <http://gcn.gsfc.nasa.gov/gcn3/4545.gcn3> (2006).
- [91] Campana, S. *et al.* GRB 060116: Swift-BAT detection of a burst. *GCN Circular* 4519, <http://gcn.gsfc.nasa.gov/gcn3/4519.gcn3> (2006).
- [92] Frail, D. GRB 060116 data. <http://www.aoc.nrao.edu/~dfrail/grb060116.dat>, (2006).
- [93] Berger, E. & Soderberg, A. M. GRB 051221: Redshift from Gemini. *GCN Circular* 4384, <http://gcn.gsfc.nasa.gov/gcn3/4384.gcn3> (2005).
- [94] Golenetskii, S. *et al.* Konus-Wind observation of GRB 051221A. *GCN Circular* 4394, <http://gcn.gsfc.nasa.gov/gcn3/4394.gcn3> (2005).
- [95] Soderberg, A. M. *et al.* The afterglow, energetics, and host galaxy of the short-hard gamma-ray burst 051221a. *Astrophys. J.* **650**, 261-271 (2006).
- [96] Hill, G., Prochaska, J. X., Fox, D., Schaefer, B. & Reed, M. GRB 051111: Keck HIRES redshift. *GCN Circular* 4255, <http://gcn.gsfc.nasa.gov/gcn3/4255.gcn3> (2005).
- [97] Yamaoka, K. *et al.* GRB 051111: Suzaku WAM observation of the prompt emission. *GCN Circular* 4299, <http://gcn.gsfc.nasa.gov/gcn3/4299.gcn3> (2005).
- [98] Frail, D. A. *et al.* GRB 051111: Radio afterglow. *GCN Circular* 4270, <http://gcn.gsfc.nasa.gov/gcn3/4270.gcn3> (2005).
- [99] Quimby, R., Fox, D., Hoefflich, P., Roman, B. & Wheeler, J. C. GRB 051109: HET optical spectrum and absorption redshift. *GCN Circular* 4221, <http://gcn.gsfc.nasa.gov/gcn3/4221.gcn3> (2005).
- [100] Tagliaferri, G. *et al.* GRB 051109: Swift detection of a burst. *GCN Circular* 4213, <http://gcn.gsfc.nasa.gov/gcn3/4213.gcn3> (2005).
- [101] Frail, D. A. *et al.* GRB 051109A. *GCN Circular* 4244, <http://gcn.gsfc.nasa.gov/gcn3/4244.gcn3> (2005).
- [102] Gal-Yam, A. *et al.* GRB 051022: host galaxy redshift. *GCN Circular* 4156, <http://gcn.gsfc.nasa.gov/gcn3/4156.gcn3> (2005).
- [103] Rol, E. *et al.* GRB 051022: Physical parameters and extinction of a prototype dark burst. *Astrophys. J.* **669**, 1098-1106 (2007).
- [104] Olive, J. *et al.* GRB 051022 (HETE 3590), A GRB detected by HETE. *GCN Circular* 4131, <http://gcn.gsfc.nasa.gov/gcn3/4131.gcn3> (2005).
- [105] Cameron, P. B. *et al.* GRB 051022: Radio counterpart. *GCN Circular* 4154, <http://gcn.gsfc.nasa.gov/gcn3/4154.gcn3> (2005).
- [106] D’Elia, V. *et al.* GRB 050922C: UVES/VLT high resolution spectroscopy. *GCN Circular* 4044, <http://gcn.gsfc.nasa.gov/gcn3/4044.gcn3> (2005).
- [107] Golenetskii, S. *et al.* Konus-Wind observation of GRB 050922C. *GCN Circular* 4030, <http://gcn.gsfc.nasa.gov/gcn3/4030.gcn3> (2005).
- [108] Frail, D. GRB 050922C data. <http://www.aoc.nrao.edu/~dfrail/grb050922c.dat> (2005).
- [109] Kawai, N. *et al.* GRB 050904: Subaru optical spectroscopy. *GCN Circular* 3937, <http://gcn.gsfc.nasa.gov/gcn3/3937.gcn3> (2005).

- [110] Cummings, J. *et al.* GRB 050904: Swift-BAT detection of a probable burst. *GCN Circular* 3910, <http://gcn.gsfc.nasa.gov/gcn3/3910.gcn3> (2005).
- [111] Frail, D. A. *et al.* An energetic afterglow from a distant stellar explosion. *Astrophys. J. Lett.* **646**, L99–L102 (2006).
- [112] Ledoux, C. *et al.* VLT/UVES spectroscopy of GRB 050820. *GCN Circular* 3860, <http://gcn.gsfc.nasa.gov/gcn3/3860.gcn3> (2005).
- [113] Page, M. *et al.* Subject: GRB 050820: Swift detection of a GRB. *GCN Circular* 3830, <http://gcn.gsfc.nasa.gov/gcn3/3830.gcn3> (2005).
- [114] Cameron, P. B. *et al.* GRB 050820A: Radio observation. *GCN Circular* 3847, <http://gcn.gsfc.nasa.gov/gcn3/3847.gcn3> (2005).
- [115] Holman, M., Garnavich, P. & Stanek, K. Z. GRB 050730, spectra and optical photometry. *GCN Circular* 3716, <http://gcn.gsfc.nasa.gov/gcn3/3716.gcn3> (2005).
- [116] Holland, S. T. *et al.* GRB 050730: Swift-BAT detection of a weak burst. *GCN Circular* 3704, <http://gcn.gsfc.nasa.gov/gcn3/3704.gcn3> (2005).
- [117] Cameron, P. B. *et al.* GRB 050730: Radio detection. *GCN Circular* 3761, <http://gcn.gsfc.nasa.gov/gcn3/3761.gcn3> (2005).
- [118] Prochaska, J. X. *et al.* GRB 050724: Secure host redshift from Keck. *GCN Circular* 3700, <http://gcn.gsfc.nasa.gov/gcn3/3700.gcn3> (2005).
- [119] Covino, S. *et al.* GRB 050724: a short-burst detected by Swift. *GCN Circular* 3665, <http://gcn.gsfc.nasa.gov/gcn3/3665.gcn3> (2005).
- [120] Berger, E. *et al.* The afterglow and elliptical host galaxy of the short γ -ray burst GRB 050724. *Nature* **438**, 988-990 (2005).
- [121] Berger, E. & Becker, G. GRB 050603: Redshift. *GCN Circular* 3520, <http://gcn.gsfc.nasa.gov/gcn3/3520.gcn3> (2005).
- [122] Golenetskii, S. *et al.* Konus-Wind observation of GRB 050603. *GCN Circular* 3518, <http://gcn.gsfc.nasa.gov/gcn3/3518.gcn3> (2005).
- [123] Cameron, P. B. *et al.* GRB 050603: Radio detection. *GCN Circular* 3513, <http://gcn.gsfc.nasa.gov/gcn3/3513.gcn3> (2005).
- [124] Foley, R. J., Chen, H., Bloom, J. & Prochaska, J. X. GRB 050525a: Gemini/GMOS Spectra. *GCN Circular* 3483, <http://gcn.gsfc.nasa.gov/gcn3/3483.gcn3> (2005).
- [125] Band, D. *et al.* GRB 050525: Swift detection of a bright, possibly short burst. *GCN Circular* 3466, <http://gcn.gsfc.nasa.gov/gcn3/3466.gcn3> (2005).
- [126] Cameron, P. B. *et al.* GRB 050525a: Radio observations. *GCN Circular* 3495, <http://gcn.gsfc.nasa.gov/gcn3/3495.gcn3> (2005).
- [127] Cenko, S. B. *et al.* GRB 050416(a): Host galaxy redshift determination. *GCN Circular* 3542, <http://gcn.gsfc.nasa.gov/gcn3/3542.gcn3> (2005).
- [128] Sakamoto, T. *et al.* Swift BAT/XRT Detection of GRB 050416. *GCN Circular* 3264, <http://gcn.gsfc.nasa.gov/gcn3/3264.gcn3> (2005).
- [129] Soderberg, A. M. *et al.* GRB 050416a: Radio detection. *GCN Circular* 3318, <http://gcn.gsfc.nasa.gov/gcn3/3318.gcn3> (2005).
- [130] Fynbo, J. P. U. *et al.* GRB 050401: VLT spectroscopic redshift. *GCN Circular* 3176, <http://gcn.gsfc.nasa.gov/gcn3/3176.gcn3> (2005).
- [131] Golenetskii, S. *et al.* Konus-Wind observation of GRB 050401. *GCN Circular* 3179, <http://gcn.gsfc.nasa.gov/gcn3/3179.gcn3> (2005).
- [132] Soderberg, A. M. *et al.* GRB 050401: Radio detection. *GCN Circular* 3187, <http://gcn.gsfc.nasa.gov/gcn3/3187.gcn3> (2005).

- [133] Kelson, D. & Berger, E. GRB 050315: Absorption redshift. *GCN Circular* 3101, <http://gcn.gsfc.nasa.gov/gcn3/3101.gcn3> (2005).
- [134] Parsons, A. *et al.* Swift-BAT detection of GRB 050315. *GCN Circular* 3094, <http://gcn.gsfc.nasa.gov/gcn3/3094.gcn3> (2005).
- [135] Soderberg, A. M. *et al.* GRB 050315: Radio afterglow. *GCN Circular* 3102, <http://gcn.gsfc.nasa.gov/gcn3/3102.gcn3> (2005).
- [136] Prochaska, J. X. *et al.* GRB 031203: Magellan spectrum of possible GRB host. *GCN Circular* 2482, <http://gcn.gsfc.nasa.gov/gcn3/2482.gcn3> (2003).
- [137] Soderberg, A. M. *et al.* The sub-energetic γ -ray burst GRB 031203 as a cosmic analogue to the nearby GRB 980425. *Nature* **430**, 648–650 (2004).
- [138] Gotz, D. *et al.* GRB 031203: A long GRB detected with INTEGRAL. *GCN Circular* 2459, <http://gcn.gsfc.nasa.gov/gcn3/2459.gcn3> (2003).
- [139] Caldwell, N., Garnavich, P., Holland, S., Matheson, T. & Stanek, K. Z. GRB 030329, optical spectroscopy. *GCN Circular* 2053, <http://gcn.gsfc.nasa.gov/gcn3/2053.gcn3> (2003).
- [140] Ricker, G. R. *et al.* GRB 030329. *IAU Circular* 8101, <http://www.cfa.harvard.edu/iauc/08100/08101.html> (2003).
- [141] Berger, E. *et al.* A common origin for cosmic explosions inferred from calorimetry of GRB030329. *Nature* **426**, 154-157 (2003).
- [142] Greiner, J. *et al.* Two absorption systems in GRB 030226. *GCN Circular* 1886, <http://gcn.gsfc.nasa.gov/gcn3/1886.gcn3> (2003).
- [143] Suzuki, M. *et al.* GRB 030226 (=U10893): A long GRB localized by the HETE WXM and SXC. *GCN Circular* 1888, <http://gcn.gsfc.nasa.gov/gcn3/1888.gcn3> (2003).
- [144] Frail, D. GRB 030226 data. <http://www.aoc.nrao.edu/~dfraile/grb030226.dat>, (2003).
- [145] Castro-Tirado, A. J. *et al.* GRB 021004: optical spectroscopy on Oct 11. *GCN Circular* 1635, <http://gcn.gsfc.nasa.gov/gcn3/1635.gcn3> (2002).
- [146] Möller, P. *et al.* Absorption systems in the spectrum of GRB 021004. *Astron. Astrophys.* **396**, L21-L24 (2002).
- [147] Shirasaki, Y. *et al.* GRB 021004(HETE 2380): A long GRB localized by HETE in near-real time. *GCN Circular* 1565, <http://gcn.gsfc.nasa.gov/gcn3/1565.gcn3> (2002).
- [148] Frail, D. A. *et al.* GRB 021004: Radio observations. *GCN Circular* 1574, <http://gcn.gsfc.nasa.gov/gcn3/1574.gcn3> (2002).
- [149] Pooley, G. GRB 021004 radio observation. *GCN Circular* 1604, <http://gcn.gsfc.nasa.gov/gcn3/1604.gcn3> (2002).
- [150] Berger, E. *et al.* GRB 021004 - VLA radio observations. *GCN Circular* 1613, <http://gcn.gsfc.nasa.gov/gcn3/1613.gcn3> (2002).
- [151] Fiore, F. *et al.* GRB 020813: High-resolution optical spectroscopy. *GCN Circular* 1524, <http://gcn.gsfc.nasa.gov/gcn3/1524.gcn3> (2002).
- [152] Villasenor, J. *et al.* GRB 020813(HETE 2262): A long, bright burst localized by HETE in near-real time. *GCN Circular* 1471, <http://gcn.gsfc.nasa.gov/gcn3/1471.gcn3> (2002).
- [153] Frail, D. A. *et al.* GRB 020813, radio detection. *GCN Circular* 1490, <http://gcn.gsfc.nasa.gov/gcn3/1490.gcn3> (2002).
- [154] Frail, D. GRB 020813 data. <http://www.aoc.nrao.edu/~dfraile/grb020813.dat> (2002).
- [155] Masetti, N. *et al.* GRB 020405: VLT spectroscopy. *GCN Circular* 1330, <http://gcn.gsfc.nasa.gov/gcn3/1330.gcn3> (2002).
- [156] Hurley, K. *et al.* IPN localization of GRB 020405. *GCN Circular* 1325, <http://gcn.gsfc.nasa.gov/gcn3/1325.gcn3> (2002).

- [157] Berger, E. *et al.* GRB 020405, Radio observations. *GCN Circular* 1331, <http://gcn.gsfc.nasa.gov/gcn3/1331.gcn3> (2002).
- [158] Gladders, M. *et al.* GRB 011211, spectrum and optical photometry. *GCN Circular* 1209, <http://gcn.gsfc.nasa.gov/gcn3/1209.gcn3> (2001).
- [159] Gandolfi, G. *et al.* BeppoSAX Alert: GRB 011211(=XRF 011211). *GCN Circular* 1188, <http://gcn.gsfc.nasa.gov/gcn3/1188.gcn3> (2001).
- [160] Frail, D. GRB 011211 data. <http://www.aoc.nrao.edu/~dfrail/011211.dat> (2001).
- [161] Garnavich, P. M. *et al.* Discovery of the low-redshift optical afterglow of GRB 011121 and its progenitor supernova 2001ke. *Astrophys. J.* **582**, 924–932 (2003).
- [162] Piro, L. *et al.* BEPOSAX GRB 011121. *GCN Circular* 1147, <http://gcn.gsfc.nasa.gov/gcn3/1147.gcn3> (2001).
- [163] Price, P. A. *et al.* GRB 011121: A massive star progenitor. *Astrophys. J. Lett.* **572**, L51–L55 (2002).
- [164] Djorgovski, S. G. *et al.* GRB 010921: Spectroscopy of the host galaxy. *GCN Circular* 1108, <http://gcn.gsfc.nasa.gov/gcn3/1108.gcn3> (2001).
- [165] Ricker, G. *et al.* HETE 1761: A bright GRB detected by HETE. *GCN Circular* 1096, <http://gcn.gsfc.nasa.gov/gcn3/1096.gcn3> (2001).
- [166] Price, P. A. *et al.* GRB 010921: Discovery of the first high energy transient explorer afterglow. *Astrophys. J. Lett.* **571**, L121–L125 (2002).
- [167] Jha, S. *et al.* GRB 010222: Another absorption line system. *GCN Circular* 974, <http://gcn.gsfc.nasa.gov/gcn3/974.gcn3> (2001).
- [168] Piro, L. *et al.* ALERT: GRB 010222: the brightest GRB observed by BeppoSAX. *GCN Circular* 959, <http://gcn.gsfc.nasa.gov/gcn3/959.gcn3> (2001).
- [169] Berger, E. *et al.* GRB 010222, radio observations. *GCN Circular* 968, <http://gcn.gsfc.nasa.gov/gcn3/968.gcn3> (2001).
- [170] Frail, D. GRB 010222 data. <http://www.aoc.nrao.edu/~dfrail/010222.dat> (2001).
- [171] Fynbo, J. P. U. *et al.* Spectroscopic redshift of GRB 000926. *GCN Circular* 807, <http://gcn.gsfc.nasa.gov/gcn3/807.gcn3> (2000).
- [172] Hurley, K. *et al.* IPN triangulation of GRB 000926. *GCN Circular* 801, <http://gcn.gsfc.nasa.gov/gcn3/801.gcn3> (2000).
- [173] Harrison, F. A. *et al.* Broadband observations of the afterglow of GRB 000926: Observing the effect of inverse Compton scattering. *Astrophys. J.* **559**, 123–130 (2001).
- [174] Price, P. A. *et al.* The unusually long duration gamma-ray burst GRB 000911: Discovery of the afterglow and host galaxy. *Astrophys. J.* **573**, 85–91 (2002).
- [175] Hurley, K. *et al.* IPN triangulation of GRB 000911. *GCN Circular* 791, <http://gcn.gsfc.nasa.gov/gcn3/791.gcn3> (2000).
- [176] Bloom, J. S., Berger, E., Kulkarni, S. R., Djorgovski, S. G. & Frail, D. A. The redshift determination of GRB 990506 and GRB 000418 with the echellete spectrograph imager on Keck. *Astron. J.* **125**, 999–1005 (2003).
- [177] Hurley, K. *et al.* IPN error box for GRB 000418. *GCN Circular* 642, <http://gcn.gsfc.nasa.gov/gcn3/642.gcn3> (2000).
- [178] Berger, E. *et al.* GRB 000418: A hidden jet revealed. *Astrophys. J.* **556**, 556–561 (2001).
- [179] Castro, S. M. *et al.* GRB 000301C: A precise redshift determination. *GCN Circular* 605, <http://gcn.gsfc.nasa.gov/gcn3/605.gcn3> (2000).
- [180] Smith, D. A. *et al.* GRB 000301C: RXTE/ASM and IPN localizations. *GCN Circular* 568, <http://gcn.gsfc.nasa.gov/gcn3/568.gcn3> (2000).

- [181] Berger, E. *et al.* A jet model for the afterglow emission from GRB 000301C. *Astrophys. J.* **545**, 56-62 (2000)
- [182] Vietri, M., Ghisellini, G., Lazzati, D., Fiore, F. & Stella, L. Illuminated, and enlightened, by GRB 991216. *Astrophys. J. Lett.* **550**, L43-L46 (2001).
- [183] Kippen, R. M. *et al.* GRB 991216: Extremely bright BATSE burst. *GCN Circular* 463, <http://gcn.gsfc.nasa.gov/gcn3/463.gcn3> (1999).
- [184] Rol, E. *et al.* GRB 991216 radio observations. *GCN Circular* 491, <http://gcn.gsfc.nasa.gov/gcn3/491.gcn3> (1999).
- [185] Frail, D. A. *et al.* The enigmatic radio afterglow of GRB 991216. *Astrophys. J. Lett.* **538**, L129-L132 (2000).
- [186] Dodonov, S. N., Afanasiev, V. L., Sokolov, V. V., Moiseev, A. V. & Castro-Tirado, A. J. GRB 991208 SAO-RAS spectroscopy. *GCN Circular* 475, <http://gcn.gsfc.nasa.gov/gcn3/475.gcn3> (1999).
- [187] Hurley, K. *et al.* IPN localization of GRB 991208. *GCN Circular* 450, <http://gcn.gsfc.nasa.gov/gcn3/450.gcn3> (1999).
- [188] Galama, T. J. *et al.* The bright gamma-ray burst 991208: Tight constraints on afterglow models from observations of the early-time radio evolution. *Astrophys. J. Lett.* **541**, L45-L49 (2000).
- [189] Harrison, F. A. *et al.* Optical and radio observations of the afterglow from GRB990510: Evidence for a jet. *Astrophys. J. Lett.* **523**, L121-L124 (1999).
- [190] Piro, L. *et al.* GRB 990510: Final BeppoSAX-WFC coordinates. *GCN Circular* 304, <http://gcn.gsfc.nasa.gov/gcn3/304.gcn3> (1999).
- [191] Kippen, R. M. *et al.* GRB 990506: BATSE Observations. *GCN Circular* 306, <http://gcn.gsfc.nasa.gov/gcn3/306.gcn3> (1999).
- [192] Taylor, G. B. *et al.* The rapidly fading afterglow from the gamma-ray burst of 1999 May 6. *Astrophys. J. Lett.* **537**, L17-L21 (2000).
- [193] Kelson, D. D., Illingworth, G. D., Franx, M., Magee, D. & van Dokkum, P. G. GRB 990123. *IAU Circular* 7096, <http://www.cfa.harvard.edu/iauc/07000/07096.html> (1999).
- [194] Kippen, R. M. *et al.* GRB 990123: BATSE Observations. *GCN Circular* 224, <http://gcn.gsfc.nasa.gov/gcn3/224.gcn3> (1999).
- [195] Frail, D. A. *et al.* GRB 990123, new radio source. *GCN Circular* 211, <http://gcn.gsfc.nasa.gov/gcn3/211.gcn3> (1999).
- [196] Kulkarni, S. R. *et al.* Discovery of a radio flare from GRB 990123. *Astrophys. J. Lett.* **522**, L97-L100 (1999).
- [197] Djorgovski, S. G., Kulkarni, S. R., Goodrich, R., Frail, D. A. & Bloom, J. S. GRB 980703: Spectrum of the proposed optical counterpart. *GCN Circular* 137, <http://gcn.gsfc.nasa.gov/gcn3/137.gcn3> (1998).
- [198] Levine, A. *et al.* GRB 980703. *IAU Circular* 6966, <http://www.cfa.harvard.edu/iauc/06900/06966.html> (1998).
- [199] Frail, D. A. *et al.* The broadband afterglow of GRB 980703. *Astrophys. J. Lett.* **590**, 992-998 (2003).
- [200] Djorgovski, S. G. *et al.* The afterglow and the host galaxy of the dark burst GRB 970828. *Astrophys. J.* **562**, 654-663 (2001).
- [201] Remillard, R., Wood, A., Smith, D. & Levine, A. GRB 970828. *IAU Circular* 6726, <http://www.cfa.harvard.edu/iauc/06700/06726.html> (1997).
- [202] Metzger *et al.* GRB 970508. *IAU Circular* 6655,

- <http://www.cfa.harvard.edu/iauc/06600/06655.html> (1997).
- [203] Metzger, M. R. *et al.* Spectral constraints on the redshift of the optical counterpart to the γ -ray burst of 8 May 1997. *Nature* **387**, 878-880 (1997).
- [204] Reichart, D. E. The redshift of GRB 970508. *Astrophys. J. Lett.* **495**, L99-L101 (1998).
- [205] Costa, E. *et al.* GRB 970508. *IAU Circular* 6649, <http://www.cfa.harvard.edu/iauc/06600/06649.html> (1997).
- [206] Frail, D. A., Waxman, E. & Kulkarni, S. R. A 450 day light curve of the radio afterglow of GRB 970508: Fireball calorimetry. *Astrophys. J.* **537**, 191-204 (2000).